4. S. A. Novikov, Yu. S. Sobolev, et al., "Investigation of the influence of the temperature on the magnitude of the fracturing stress during spall in copper," Probl. Prochn., No. 3 (1977).
5. B. M. Butcher, L. M. Barker, D. E. Munson, and C. D. Lundergan, "Influence of stress history on time-dependent spall in metals," AIAA J., 2, No. 6 (1964).
6. B. A. Tarasov, "Resistance to fracture of plates under shock loading," Probl. Prochn., No. 3 (1974).
7. F. A. Baum, L. P. Orlenko, K. P. Stanyukovich, V. P. Chelyshev, and B. I. Shekhter, Physics of Explosion [in Russian], Nauka, Moscow (1975).
8. L. Seaman, D. R. Curran, and D. A. Shockey, "Computational models for ductile and brittle fracture," J. Appl. Phys., 47, No. 11 (1976).

DEPENDENCE OF THE CRITICAL STRESSES ON THE LOADING TIME PARAMETERS DURING SPALL IN COPPER, ALUMINUM, AND STEEL

V. I. Romanchenko and G. V. Stepanov UDC 620.17

Intensive shock and explosive pulse loads, used extensively in a number of modern engineering areas, result in the origination of a specific kind of fracture, called spall, in the construction material which is caused by the appearance of tensile stresses during interaction of opposing loading waves [1-4].

In this connection, an investigation of the operability of materials, and the clarification of those conditions under which they do not fracture under the action of pulse loads, are of practical interest. The independent scientific interest in the investigation of spall is due to the possibility of setting up a strength-time relation for short-range actions (to 10^{-7} sec) of high stress levels.

The development of loading facilities and methods of recording parameters behind shocks (precisely there does spall occur), and the application of continuous recording methods [5-8] permit advancement in this area. From the authors' viewpoint, investigations [9] using laser interferometers permitting the experimental recording of the wave profile during loading and determination of the force and time characteristics of the spalling fracture thereby, were substantial progress. However, use of an acoustic approximation by the authors of this paper during processing of the experimental data should apparently be considered just the first step to obtaining the information needed. In the pressure range to 150 kbar, as is known, the shocks are elastic–plastic in nature in the majority of structural materials for which the presence of an elastic part, an elastic predecessor, anda plastic wave being propagated at different velocities, is characteristic. The acoustic approximation does not take this circumstance into account and can induce a significant error, especially in determining the load time parameters [8]. Moreover, knowledge of experimentally determined properties of the materials used as parameters in these problems is necessary for a numerical examination of the different problems associated with the elastic–plastic wave propagation and the fracture of the bodies ([10], for instance). Hence, the appropriate models of the medium should be used in processing the experiments.

A method and the results of determining the load force and time characteristics during the spalling fracture of copper, the aluminum alloy B95, and steel subjected to the action of plane shocks of intensity up to 160 kbar, are presented in this paper. The material is considered an elastic–plastic body under loading and unloading.

Because of the practical impossibility of recording the load parameters in the spall domain, they are assessed by means of the change in state on the interface of the material being tested and a material of low dynamic stiffness. The diagram of the experiment is represented in Fig. 1. The impactor 1 of 90-mm diameter was accelerated in an air-passage apparatus assuring extreme planarity of the collision, to a velocity V_0 of around 900 m/sec, t–x

Kiev. Translated from Zhurnal Prikladnoi Mekhaniki i Tekhnicheskoi Fiziki, No. 4, pp. 141-147, July-August, 1980. Original article submitted September 4, 1979.

0021-8944/80/2104-0555$07.50

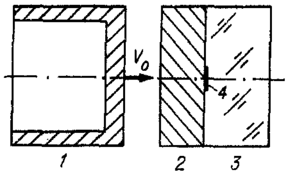

Fig. 1

and p–U diagrams of wave interaction in the specimen 2 are represented in Fig. 2 (t is the time, x is the coordinate, p is the stress normal to the wave front, and U is the mass flow rate). Domains in the t–x diagram correspond to the points in the p–U plane. To produce opposing unloading waves in the specimen which are capable of causing fracture during interaction, the impactor material should have a smaller or similar dynamical stiffness relative to the specimen; the "soft" material 3 (Fig. 2) has a considerably lower dynamical stiffness. For this reason the impactor was fabricated from aluminum or from steel, while organic glass was used as the "soft" material. A dielectric transducer 4 that permitted continuous recording of the pressure change behind the shocks for a long time (around 10 μsec) [8] was used for the recording. A typical test oscillogram and photograph of the specimen with spall are presented in Figs. 3a and b. The stress profile on the specimen–organic glass interface, following from the t–x and p–U diagrams, is presented in Fig. 4. The time t_1 corresponds to arrival of the shock at the interface, t_2 to arrival of the unloading wave from the rear surface of the impactor, while the time t_3 is associated with reaching the critical stresses σ_{cr} in the spall plane (the maximal tensile stresses are understood to be critical). Knowing the magnitude of the stresses at the points 1, 5, 6, the shock adiabats and unloading isentropes of the appropriate materials, we can determine the magnitude of the stress σ_{cr} during fracture. As is seen from Fig. 2a change in stress from the shock compression pressure p_a to the critical magnitude of the tensile stresses occurs in the spall plane when neglecting the curvature of the characteristics during the time $\Delta t = t_3 - t_2$. Therefore, the mean rate of load change in the spall plane

$$\left(\frac{dp}{dt}\right)_0 = \frac{|p_a| + |\sigma_{cr}|}{\Delta t}$$

and the strain rate

$$\dot{\varepsilon} = \frac{1}{\rho D^2}\left(\frac{dp}{dt}\right)_0,$$

can be estimated from the oscillogram, where ρ is the density, and D is the shock velocity.

As experiments have shown, a shock in steel and aluminum has an obvious elastic–plastic configuration. Since the stresses being measured are comparable to the Hugoniot elastic limit p_y, the material behavior was described by the theory of elastic–plastic strain. Under loading the material is initially deformed elastically to the point A (Fig. 5), then plastically to the point B corresponding to the shock compression pressure, under unloading from the point B, elastically on the section BC, and then plastically to the magnitude of the critical stresses. The line AB exceeds the hydrodynamic compression line by $(2/3)\sigma_T$ = const, i.e., the diagram of ideal elasticity–plasticity is taken (the Bauschinger effect is neglected). Magnitudes of the stresses in the elastic and plastic waves are computed from the known relationship $\Delta p = \rho D \Delta U$. In the elastic domain D = 6.1 km/sec for steel, D = 6.4 km/sec for aluminum, and 5.05 and 5.5 km/sec, respectively, in the plastic domain. No elastic properties were detected in copper even at low shock compression pressures; consequently, the hydrodynamic compressibility model with D = 4.15 km/sec was taken for it. Their mean values in the pressure range investigated were taken as plastic wave velocities in aluminum and copper. The deviation from the mean did not exceed 5% for both metals.

Since the material starts to be deformed in the reverse direction during fracture (there had been tension, compression starts), then the more rapid propagation of the spalling pulse over the thickness of the spall layer of the elastic part results in its shift relative to the unloading wave represented by a family of C_+ - characteristics, whereupon an earlier change in stress occurs, and the stress on the specimen–organic glass interface p_1 turns out to be exaggerated as compared with that which would correspond to σ_{cr} at the point M. We then represent the quantity σ_{cr} as the sum

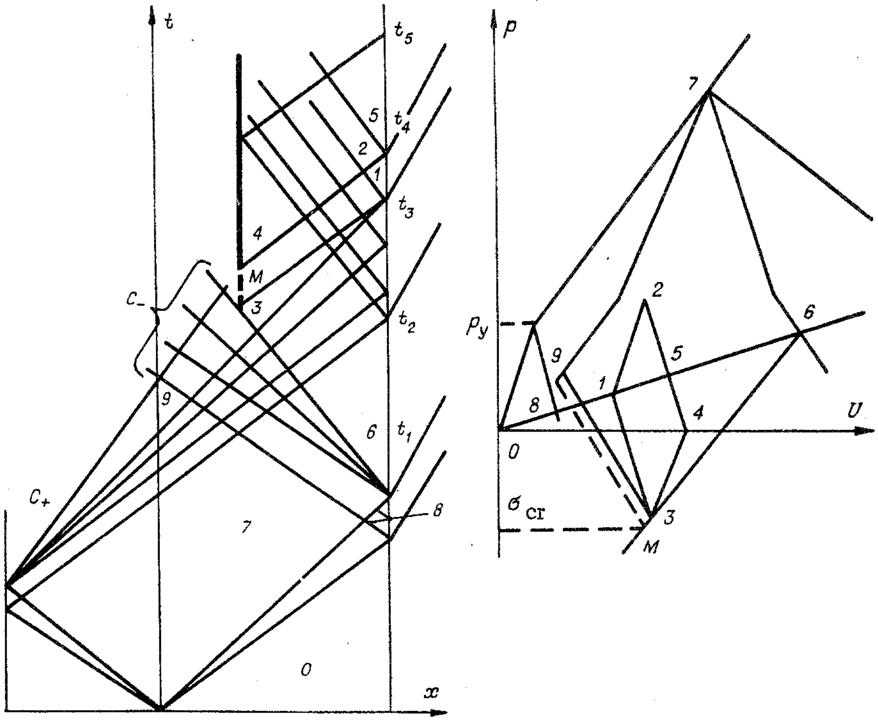

Fig. 2

$$\sigma_{cr} = \sigma_3 + \Delta\sigma,$$

where σ_3 is the magnitude of the tensile stresses at the point 3, where it is calculated by using the formula

$$\sigma_3 = (\alpha p_1 + p_6 + \rho D_p(U_1 - U_6))/(1 + \alpha), \ \alpha = D_p/D_e,$$

which is valid for $\sigma_{cr} < 2p_e$ and $p_\alpha > 2p_e$, otherwise the lines 6-3 and 1-3 (see Fig. 2) are bilinear; D_e and D_p are the elastic and plastic wave velocities in the material under investigation, U_1 and U_6 are the mass flow rates in the "soft" material under the pressures p_1 and p_6, respectively (agreement of the unloading isentrope with the shock adiabat in p–U coordinates was taken for the organic glass; information about the compressibility of organic glass was taken from [11]); $\Delta\sigma$ is the stress change in making the transition from point 3 to point M:

$$\Delta\sigma = \frac{1}{2}\left(\frac{dp}{dt}\right)_p \delta\left(\frac{1}{C_p} - \frac{1}{D_e}\right),$$

where $(dp/dt)_p$ is the rate of change in the stress along the "tail" of the C_- -characteristic, $(dp/dt)_p = (|p_6| + |\sigma_3|)/0.5\ \Delta t$; C_p is the propagation velocity of the perturbation along the C_+-characteristic passing through the point M (its magnitude is determined experimentally from the test oscillogram. It is usually close to the plastic wave velocity), and δ is the spall thickness.

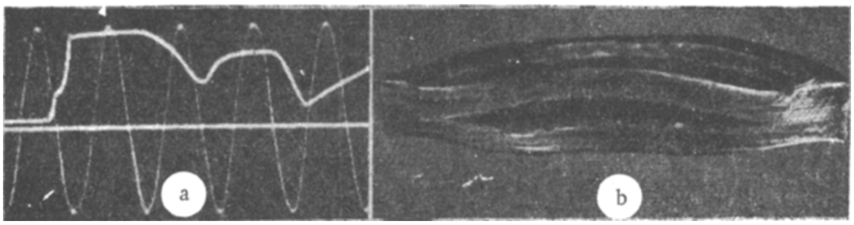

Fig. 3

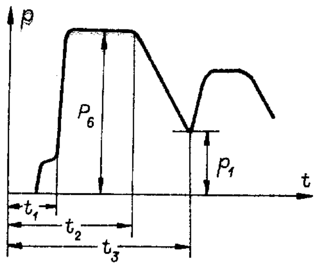

Fig. 4

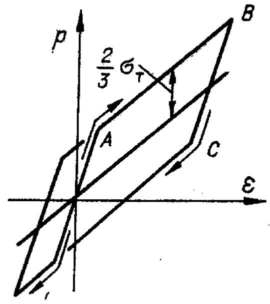

Fig. 5

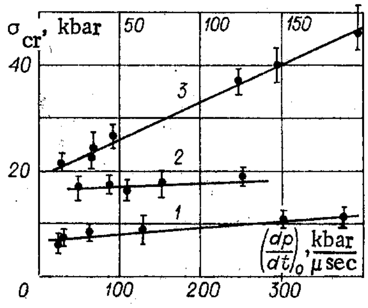

Fig. 6

The time of tensile stress growth from zero to σ_{cr}

$$t_t = \sigma_{cr} \bigg/ \left(\frac{dp}{dt}\right)_0.$$

can be determined from the rate of load change in the small plane. Direct measurement of t_t was performed in experiments by the "artificial" spall scheme, whose crux is to assure zero tensile strength of the material in the plane of the assumed spall in the test. The location of this latter was determined in the test in a complicated manner, then an identical specimen was slit along the spall plane and the same test was performed. Comparing oscillograms with a continuous record of the parameters behind the shock front in either case permits the experimental determination of t_t.

The results of the investigations are presented in Fig. 6 (1 is for copper; 2 for aluminum, and 3 for steel; the upper scale is for aluminum), and also in the table. Data averaged over 2-4 tests are presented in the table. The time for the tensile stresses to drop from σ_{cr} to zero t_d was determined by the time to reach the maximum pressure in the spall pulse. Variation of the rate of change in load was executed by changing the thickness of the impactor-specimen pair and the collision velocity. The organic glass thickness was chosen so that the unloading wave from its free surface would not affect the measurement. The maximum specimen thickness used in the tests was constrained by the condition of one-dimensionality of the strain during the whole recording time (t_4 in Fig. 2). Special tests, in which the impactor was taken sufficiently thick to assure earlier arrival of the side unloading at the transducer as compared with the rear unloading from the impactor, were conducted to determine this time. The times of the beginning of the pressure drop behind the shock front were measured, which were also taken as the time of one-dimensionality of the strain. The specimen minimum thickness was selected so as to assure damping of processes associated with viscosity of the material. It is known [12] that the influence of viscosity due to the high strain rate is most substantial close to the collision surface. An experimental study of elastic predecessor attenuation in small steel and aluminum thicknesses [13, 14] permitted establishment of the last allowable specimen thickness in the experiments, which was 10 mm.

As the collision velocity V_0 diminished, the time when there was no fracture set in for each of the metals. The maximal tensile stresses in the specimen $\sigma*$ and the time of their action were determined from the oscillograms for such cases. Checking on the presence or absence of fracture was by microscopic observation of cuts from specimens subjected to loading. A 100-fold enlargement usually turned out to be sufficient for macrocrack detection. The stress at which there was no mainline crack was taken as $\sigma*$.

TABLE 1

v_0, m/sec	Mater. of impactor–spec. pair	Thickness, mm: impactor	Thickness, mm: spec.	$\left(\frac{dp}{dt}\right)_0$, kbar/μsec	t_p, μsec (comp.)	σ_{cr}, σ_*, kbar	t_p, μsec ("artif." spall)	t_c, μsec
224	AL–ST	10	15	—	—	15,2	—	—
358	ST–ST	2	10	238	0,16	37,2	—	0,1
383	AL–ST	10	15	63	0,35	22,1	0,32	0,27
400	»	10	40	38,5	0,56	21,3	0,6	1,2
455	»	10	15	91,5	0,29	26,6	0,26	—
580	ST–ST	5	10	296	0,14	40,0	—	—
588	»	2	10	392	0,12	45,2	0,1–0,15	0,1
870	AL–ST	10	40	67	0,37	24,5	—	~1
200	AL–AL	10	15	—	—	10,2	—	—
328	»	10	15	43	0,40	17,2	0,34	0,55
380	»	10	15	55	0,29	16,0	0,33	0,65
450	»	10	40	20,5	0,82	16,8	0,68	1,8
633	»	10	15	72	0,24	17,5	—	0,35
760	»	4,3	10	123	0,15	18,4	0,15	0,5
78	AL–M	10	15	—	—	5,5	—	—
163	»	10	15	28	0,21	5,9	0,19	1,9
225	»	10	15	32	0,23	7,3	0,25	2,0
400	»	10	15	65	0,13	8,45	0,1–0,15	1,0
533	ST–M	2	10	300	0,034	10,2	—	0,45
762	AL–M	10	15	124	0,07	8,7	—	0,65
780	ST–M	5	15	370	0,03	11,1	<0,1	0,37

Note: AL) aluminum; ST) steel; M) copper. In aluminum p_e = 5.5 kbar and in steel p_e = 9.5 kbar.

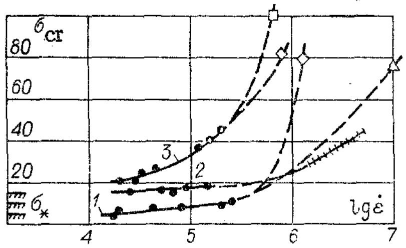

Fig. 7

As is seen from the results presented, the influence of the loading rate is most essential in steel, and refers to a lesser degree to copper also. The strength of aluminum (the alloy B95) depends slightly on the loading rate. Such a dependence is observed qualitatively in quasistatic tests also [8].

Comparing the results obtained with the numerous data of other researchers is sufficiently complicated because, with rare exceptions ([10], for instance), direct experimental measurements of the shock profile were not performed in the majority of papers. The following must hence be noted.

The development of spall in materials occurs because of the interaction of two opposing unloading waves. When using the stress gradient or the rate of stress change only behind the incident wavefront as the time characteristic, the influence of these parameters behind the reflected unloading wave front on the nature of the load change at the fracture site is not taken into account. Evidently, the rate of pressure change and the pressure gradient in the material are lowered (the characteristics diverge) as the unloading wave is propagated over it, hence, the rate of load change in the spall plane depends on the path transversed by both the incident and the reflected waves, i.e., on the thickness of the impactor–specimen pair and on the thickness of the spall.

It is seen from the symmetric pattern in the domain of interaction of two opposing unloading waves that the state parameters in two symmetrically disposed points belonging to the last C_+ and C_--family characteristics are perfectly identical. Conditions for spall occur simultaneously on the last C_+ and the last C_--characteristics. The fracture condition is satisfied between these points since the tensile stresses here are large. An analogous pattern holds also for the nonsymmetric interaction of unloading waves. This can be explained by the presence of friability, the intensive fracturing in the domain adjoining the spall, as detected in a number of papers [15-17]. It follows from simple computations that the width of the unloading wave interaction domain during the collision of plates has a dimension on the order of 1 mm depending on the thickness of the impactor, the specimen, and the spall. The tensile stresses at points belonging to this domain vary between zero and $-p_a$. Consequently, the accuracy in measuring the spall thickness strongly affects the computation of the critical stresses determined in a number of papers on its magnitude. This, as well as the absence of direct recording of the shock profile during spall can explain the considerable spread in the experimental data for identical materials, which sometimes differ by an order of magnitude [18, 19]. The use of oscillograms with a continuous record of the change in state parameters behind the shock front and a suitable selection of the material behavior model is capable of yielding objective information about the magnitudes of the acting stresses and of the load time parameters during spalling fracture.

Results of the present paper on the order of magnitude of the critical stresses agree with the data for steel in [2, 3, 20, 21], for copper in [2, 9, 18], and for aluminum in [2, 9, 20, 22]. The results on aluminum [23], steel [24, 25], and copper [3, 25], and the results of this paper show that σ_{cr} grows as $\dot{\varepsilon}$ increases (Fig. 7). The asymptote on the σ axis is the quantity σ_*, the stress below which spall in the material is absent for ∿2 μsec. More accurately, the body is not separated into two parts although the individual cracks are observed in the material. The difference between the results in this paper and in [9] can be explained by the difference in the time parameters used to construct the dependence, as well as by the possible influence of flow inhomogeneity behind the shock front on the measurements in [9].

The authors are grateful to V. V. Astanin and G. T. Rudek for aid in performing the experiments.

LITERATURE CITED

1. B. M. Butcher, L. M. Barker, D. E. Munson, and B. M. Lundergan, "Influence of stress history on time-dependent spall in metals," AIAA J., No. 2 (1964).
2. F. F. Vitman, M. I. Ivanov, and B. S. Ioffe, "Resistance of plastic materials to fracture under pulse loading," Fiz. Met. Metalloved., 18, No. 5 (1964).
3. S. A. Novikov, I. I. Divnov, and A. G. Ivanov, "Investigation of the fracture of steel, aluminum, and copper under explosive loading," Fiz. Met. Metalloved., 21, No. 4 (1966).
4. B. A. Tarasov, "On the time dependence of organic glass strength under shock loading," Probl. Prochn., No. 12 (1972).
5. G. I. Kanel', "Application of manganin transducers to shock compression pressure measurements of condensed media," Preprint Inst. Fiz. Khim. Akad. Nauk SSSR, Chernogolovka (1973).
6. N. A. Zlatin, S. M. Mochalov, G. S. Pugachev, and A. M. Bragov, "Laser differential interferometer," Zh. Tekh. Fiz., 43, No. 9 (1973).
7. S. A. Novikov and A. G. Ivanov, "Capacitive transducer method to record the instantaneous velocity of a moving surface," Prib. Tekh. Eksp., No. 1 (1963).
8. G. V. Stepanov, Behavior of Structural Materials in Elastic—Plastic Loading Waves [in Russian], Naukova Dumka, Kiev (1978).
9. N. A. Zlatin, S. M. Mochalov, G. S. Pugachev, and A. M. Bragov, "Time regularities of fracture under intensive loads," Fiz. Tverd. Tela, 16, No. 6 (1974).
10. L. D. Bertholf, Buxton, et al., "Damage in steel plates from hypervelocity impact. II. Numerical results and spall measurement," J. Appl. Phys., 46, No. 9 (1975).
11. D. N. Schmidt and M. W. Evans, "Shock wave compression of Plexiglas in 2.5 to 20 kbar region," Nature, 206, 1348 (1965).
12. V. N. Kukudzhanov, "Elastic—plastic wave propagation in a rod taking account of the influence of the strain rate," Tr. Vychisl. Tsentr Akad. Nauk SSSR (1967).
13. V. V. Astanin, G. V. Stepanov, and V. I. Romanchenko, "Resistance to shear in metals behind a shock front," in: Abstracts of Reports, Second All-Union Sympos. on Pulse Pressures [in Russian], Moscow (1976).
14. J. W. Taylor, "Dislocation dynamics and dynamics yielding," J. Appl. Phys., 36, 3146 (1965).
15. V. V. Adushkin and A. P. Sukhotin, "On fracture of a solid medium by explosion," Prikl. Mekh. Tekh. Fiz., No. 4 (1961).
16. B. M. Butcher, "Spallation in 6061-T6 aluminum," in: Sympos. H.D.P., Paris (1967).

17. V. I. Romanchenko and G. V. Stepanov, "On the question of the time dependence of the strength of solids under spall," Probl. Prochn., No. 3 (1978).
18. J. H. Smith, "Three low pressure spall thresholds in copper," ASTM STP, Vol. 336 (1963).
19. R. C. McQueen and S. R. Marsh, "Ultimate yield strength of copper," J. Appl. Phys., 33, 654 (1962).
20. D. Reinhart and D. Pearson, Metal Behavior under Impulsive Loads [Russian translation], Moscow, IL (1958).
21. J. S. Buchanan and H. J. James, "Measurement of high intensity stress pulses," Brit. J. Appl. Phys., 10, 290 (1959).
22. Response of Metals to High Velocity Deformation, Interscience (1960).
23. S. A. Novikov and L. M. Sinitsyna, "On the influence of the strain rate during spall on the magnitude of the fracturing stresses," Fiz. Met. Metalloved., 28, No. 6 (1969).
24. I. Skidmore, "Shocks in solids," in: Topics in Mechanics [Russian translation], No. 4, (1968).
25. Yu. I. Tarasov, "Investigation of the dependence of the fracture time on the tensile load for steel and copper," Dokl. Akad. Nauk SSSR, 165, No. 5 (1965).

VARIATIONAL FORMULATIONS OF BOUNDARY-VALUE PROBLEMS IN MATERIAL FAILURE

A. F. Revuzhenko

UDC 539.375

In [1] we considered the formulation of boundary-value problems in the deformation of materials which possess the property of localizing slip. In the present article we consider variational formulations for the general case of material failure, when there are severe discontinuities both in the tangential and in the normal components of the displacements.

1. We shall confine our attention to the case of plane deformation or a plane stressed state. We introduce the cartesian coordinates Ox_1x_2. We denote by S the deformed region bounded by the contour Γ. Suppose that for specified load parameters the region is divided by a line of severe discontinuity of the displacements. Hereafter, it will be sufficient to confine our attention to the case of a single line. The results remain valid for the case of several lines. We assume first of all that the trajectory of the distribution of the lines is known either from experimental data or from symmetry conditions, or that it is given on the basis of additional concentrations. For one rather broad class of models the boundary-value problem of the propagation of the discontinuity lines and the deformation of the material outside the lines can be reduced to the determination of the stationary values of certain functionals on the class of discontinuous functions. The functionals must depend both on the behavior of the functions in the region of smoothness and on the value of the discontinuities of these functions. Suppose that in S there are given certain fields of stresses σ_{ij}, displacements u_k, and variables $\lambda_r (i, j, k = 1, 2, r = 1, 2, \ldots)$. We define the functional

$$W = \int\limits_{S^+} F\left(u_i^+, u_{i,i}^+, \gamma^+, \sigma_{ij}^+, \sigma_{ij,k}^+, \lambda_r^+, \lambda_{r,k}^+, x_k\right) dx_1 dx_2 + \int\limits_{S^-} F\left(u_i^-, \ldots\right) dx_1 dx_2 + \int\limits_L U dl - \int\limits_\Gamma \Pi dl, \tag{1.1}$$

where $\lambda = u_{1,2} + u_{2,1}$; $\sigma_{12} = \sigma_{21}$; U, Π are functions defined on the line of discontinuity L and the external boundary. Here and hereafter, a comma before a subscript denotes differentiation with respect to the appropriate coordinate, and the superscripts +, −, indicate the notation in the regions to the right and left of L. We assume that on real solutions the functional is stationary. We consider the formulation when all equations are completely determined by the variational principle, and consequently there are no other limitations within S^+, S^-. The necessary condition for an extremum leads to the following system of Euler–Ostrogradsky equations:

Novosibirsk. Translated from Zhurnal Prikladnoi Mekhaniki i Tekhnicheskoi Fiziki, No. 4, pp. 148-156, July-August, 1980. Original article submitted October 15, 1979.

